

Analyst

Accepted Manuscript



This is an *Accepted Manuscript*, which has been through the Royal Society of Chemistry peer review process and has been accepted for publication.

Accepted Manuscripts are published online shortly after acceptance, before technical editing, formatting and proof reading. Using this free service, authors can make their results available to the community, in citable form, before we publish the edited article. We will replace this *Accepted Manuscript* with the edited and formatted *Advance Article* as soon as it is available.

You can find more information about *Accepted Manuscripts* in the [Information for Authors](#).

Please note that technical editing may introduce minor changes to the text and/or graphics, which may alter content. The journal's standard [Terms & Conditions](#) and the [Ethical guidelines](#) still apply. In no event shall the Royal Society of Chemistry be held responsible for any errors or omissions in this *Accepted Manuscript* or any consequences arising from the use of any information it contains.

PAPER

Sensitive impedimetric biosensor based on duplex-like DNA scaffolds and ordered mesoporous carbon nitride for silver(I) ion detection

Cite this: DOI: 10.1039/x0xx00000x

Received 00th January 2012,

Accepted 00th January 2012

DOI: 10.1039/x0xx00000x

www.rsc.org/Yaoyu Zhou^{ab}, Lin Tang^{*ab}, Xia Xie^{ab}, Guangming Zeng^{*ab}, Jiajia Wang^{ab}, Yaocheng Deng^{ab}, Guide Yang^{ab}, Chen Zhang^{ab}, Yi Zhang^{ab} and Jun Chen^{ab}

This study demonstrates a new unlabeled immobilized DNA-based biosensor with ordered mesoporous carbon nitride material (MCN) for detection of Ag⁺ by electrochemical impedance spectroscopy (EIS) with [Fe(CN)₆]^{4-/3-} as redox couple. The unlabeled immobilized DNA initially formed the hairpin structure through hybridization with the probe, and then changed to duplex-like structure upon interaction with Ag⁺ in solution to form a C–Ag⁺–C complex at electrode surface. As a result, the interfacial charge-transfer resistance of the electrode towards the [Fe(CN)₆]^{4-/3-} redox couple was changed. Thus, a declined charge transfer resistance (*R_{ct}*) was obtained, corresponding to Ag⁺ concentration. MCN provide an excellent platform for DNA immobilization and faster electron transfer. Impedance data were analyzed with the help of Randles' equivalent circuit. The lower detection limit of the biosensor for Ag⁺ is 5 × 10⁻¹¹ M with good specificity. All the results showed that this novel approach provides a reliable method for Ag⁺ detection with sensitivity and specificity, potentially useful for practical applications. Moreover, other DNA detection methods for more heavy metals may derive from this idea and applied in the environmental field.

Introduction

Silver(I) ions are recognized as one of the most hazardous metal pollutants due to their potential toxicity to human health and the environment, surpassed only by mercury¹. They are mostly generated from photographic and imaging industry, dental and medical products, electrical and electronic equipments, and other products like jewelry, coins, and mirrors². Their toxicity may accumulate in the human body through the food chain or directly drinking, bringing on undesirable seriously damage problems, such as cytotoxicity, organ failure and reduction in mitochondrial function³. Thus, it is of great significance to monitor its level in natural water environment worldwide. Traditional quantitative methods, such as electrothermal atomic absorption spectrometry (ETAAS)⁴, inductively coupled plasma mass spectrometry⁵, and cold vapor atomic fluorescence spectrometry (CVAFS)⁶, have been extensively applied to detect heavy metal ions with high sensitivity. In addition to the time consuming process, expensive and complex instrumentations, these techniques normally involve sophisticated chemical procedures for extracting metal ions from samples, in which the speciation change of metal ions is unavoidable⁷.

In the past decade, many efforts have been focused on the design of DNA-based biosensors to detect metal ions based on interactions between some metal ions and the nucleic acids to form stable metal-mediated DNA duplexes⁸. For example, mercury ions (Hg²⁺) are capable of selectively coordinating thymine (T) bases to form stable T–Hg²⁺–T complexes⁹. For Pb²⁺ detection, most sensors are based on the Pb²⁺-dependent

DNAzyme and the Pb²⁺-stabilized G-quadruplex¹⁰. Besides, since Ono *et al.* found that Ag⁺ can selectively coordinate cytosine (C) bases to form stable C–Ag⁺–C complex and discussed the mechanism of the specific interactions between silver(I) ions and cytosine–cytosine pairs¹¹, various detection techniques such as fluorescence, surface-enhanced Raman spectroscopy, resonance scattering, colorimetry and electrochemical methods were applied to selectively detect Ag⁺ in aqueous media by taking advantage of specific C–Ag⁺–C interaction and signal amplification of nanomaterials^{11–13}. Accordingly, various detection techniques were applied to selectively detect these heavy metal ions based on hairpin structure DNA biosensor^{11,14–15}. Compared to linear DNA structures, hairpin structure DNA biosensors have higher detection sensitivity and stability¹⁶, generally specific to a given ligand–biomolecule interface and mostly insensitive to other molecules even in complex environments (natural water, living cells, or blood serum) owing to their highly constrained conformations¹⁷, which may improve the potential application in real environment. Moreover, an effective immobilization platform for the DNA scaffold is also a key issue in the detection system. To date, various nanomaterials, such as GNPs/carbon nanodots¹⁸, single-walled carbon nanotubes (SWCNTs)¹⁹, carbon nanotube (CNT)²⁰, porous materials (micropores (<2 nm), mesopores (2–50 nm) and macropores (>50 nm))^{21,22}, have been successfully exploited for an effective platform for sensors relying on different transduction schemes. In our previous study, we used ordered mesoporous carbon nitride (MCN) as the platform for electrochemical biosensors, which can obviously increase the sensitivity and lower the

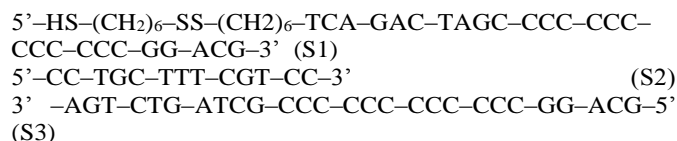
detection limit²³, MCN has better microenvironment for immobilized biomolecules due to the CN matrix, higher affinity for bioactivator, and faster electron transfer between bioactivator and MCN-sensing sites because of the π - π^* electronic transition in the MCN.

This study developed a novel impedimetric hairpin structure DNA biosensor with MCN for the ultrasensitive detection of Ag⁺. The interfacial charge-transfer resistance of the DNA/MCH/GNPs-MCN/L-Lys-modified electrode will change upon the hybridization of surface-tethered probe DNA with its complementary DNA and interaction with Ag⁺ in solution, which could be useful for practical determination of Ag⁺.

Experimental

Chemicals and Reagents

Pluronic copolymer P123 (EO20PO70EO20, EO=ethylene oxide, PO=propylene oxide), Tris (hydroxymethyl) aminomethane, were purchased from Sigma-Aldrich (USA). Gold (III) chloride trihydrate (HAuCl₄·3H₂O, 99.9%) was purchased from Dingguo Biotechnology Co., Ltd (Shanghai, China). Tetraethoxysilane (TEOS), K₃[Fe(CN)₆], K₄[Fe(CN)₆], L-Lysine (L-Lys), AgNO₃, NaClO₄, and all other chemicals were of analytical grade and used as received. And all aqueous solutions were prepared using ultra-pure water (18 M Ω ·cm, Milli-Q, Millipore). Tris-ClO₄ buffer (pH=7.4) containing 300 mM NaClO₄ and phosphate buffer saline (PBS, 0.1 M KH₂PO₄ and 0.1 M Na₂HPO₄) were used in this work. The DNA target-specific probes used for hybridization in our experiment were synthesized by Sangon (Shanghai, China) and purified using high-performance liquid chromatography. The sequences of the oligonucleotides include:



Apparatus

Cyclic voltammetric (CV) measurement and electrochemical impedance spectroscopy (EIS) measurements were carried out on CHI760D electrochemical workstation (Chenhua Instrument, Shanghai, China). The three-electrode system used in this study consisted of a modified electrode as working electrode, a saturated calomel electrode (SCE) as reference electrode and a Pt foil auxiliary electrode. The solution pH was measured with a model pHSJ-3 digital acidimeter (Shanghai Leici Factory, China). Scanning electron microscopy (SEM) images were obtained using a JSM-6360LV field emission scanning electron microscope. Transmission electron microscopy (TEM) images were obtained on a JEOL-1230 electron microscope operated at 100 kV. A Sigma 4K15 laboratory centrifuge, a vacuum freezing dryer and a mechanical vibrator were used in the assay.

Sensor fabrication

The MCN was synthesized in our laboratory as described previously²³. The bare glass carbon electrode (GCE) used for

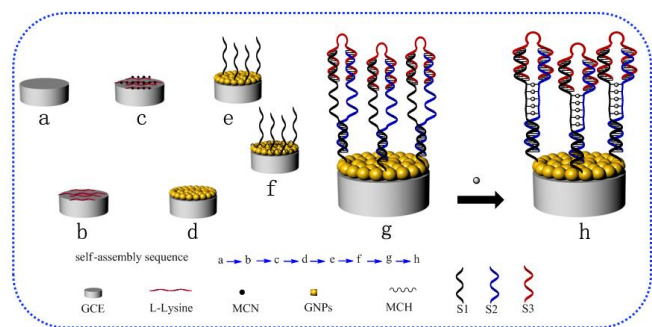
the self-assembled monolayer was first polished in alumina slurry, rinsed with deionized water, and then etched for about 10 min in a "Piranha" solution (98% H₂SO₄:30% H₂O₂ = 3:1 (v/v)) to remove organic contaminants (*Caution: Piranha solution reacts violently with organic materials, thus should be handled with extreme care.*)²³⁻²⁵. Finally, the electrode surface was treated by cyclic voltammetry scan in 0.5 M H₂SO₄ between 0 and 1.2 V at the scan rate of 50 mV s⁻¹ until a reproducible scan was obtained.

MCN suspension was prepared by dispersing 1 mg purified MCN into 1 mL N,N-dimethylformamide with the aid of ultrasonic agitation. The preparation of GNPs-MCN/L-Lysine/GCE was carried out as follows (as shown in Scheme 1): initially, the L-Lys film modified electrode was obtained in L-Lys electrodeposition process (as seen in Fig. S-1). Then, a 5.0 μ L of the MCN dispersion was dipcoated onto L-Lysine/GCE. The electrode (MCN/L-Lysine/GCE) was dried at room temperature (25 °C) for about an hour. The GNPs were immobilized on the pretreated electrode (MCN/L-Lysine/GCE) by electrodepositing gold(III) chloride trihydrate (HAuCl₄·3H₂O), and the method of electrodeposition was used according to the previous description in our laboratory²⁴. Subsequently, the mixture solution of 10 μ L S1 probe was dropped onto the electrode surface and kept at 4 °C for self-assembling through thiol-gold bonding for 10 h. The hybridization of the biosensor is as follows. The modified electrode with S1 probes coated was immersed into 400 μ L of 6-mercapto-1-hexanol (MCH) solution for 1 h to improve the quality and stability, to reduce nonspecific adsorption of DNA and to obtain a well aligned DNA monolayer. Then, the electrode was soaked in the 2.5 μ M DNA solution containing S2 and S3 (1:1), and incubated at room temperature for 1 h to form the hairpin structured (S1+S2+S3). Subsequently, it was washed with Tris-ClO₄ buffer (pH=7.4). When not in use, the electrode was stored in a moist state at 4 °C.

Design of biosensing strategy

Scheme 1 outlines the preparation processes of the duplex-like DNA scaffolds biosensor. Here, MCN was synthesized and applied to fix DNA through Au nanoparticle (GNPs) films, as a transducer to convert the recognition information into a detectable signal. GNPs were also employed to amplify the detectable signal, which can also easily and directly couple mercapto biomolecules with no more modification. L-Lysine (L-Lys) was also used for its non-toxicity, biocompatibility, and good film-forming ability. First, MCN enriched in amino and carboxy groups could be immobilized on the electrode surface by linking the -NH₂ and -COOH of L-Lys through amino-carboxyl bonding²³, and used as carrier for loading DNA labels and accelerating electron-transfer. The spatial structure of the MCN/GNPs offered more reaction sites and space for self-assembly of the DNA probe because of the CN matrix, and CN matrix has many prominent properties, especially, the presence of basic sites, affinity for biomolecules and larger bioactivity after entrapment procedure²³, which are

important for biosensor performance. Second, the use of low concentration L-Lys protected the link between MCN/GNPs and GCE by forming a film. They can make the MCN/GNPs film fixed more tightly through its amino-carboxyl as molecular bridge. And this method might extend the using life and stability of the biosensor. Third, the film structure of MCH on the electrode surface was similar to the reported function of chitosan²⁶ and Polyethylene glycol (PEG)²⁷, weakening unspecific adsorptions, strengthening the orientation of the thiolated DNA probe, and facilitating the hybridization process²⁸. Though L-Lys and MCH reduced electric conductivity and blocked the electron transfer processes at the electrode surface, their advantages outweighed the disadvantages here.



Scheme. 1 The fabrication processes of the duplex-like DNA scaffolds biosensor.

Detection process

The electrode reacted with various concentrations of Ag^+ in buffers (Tris- ClO_4 buffer, pH 7.4) for 2 h. Subsequently, it was washed with Tris- ClO_4 buffer (pH=7.4). A conventional three-electrode system was used, and all the measurements were carried out at room temperature. Electrochemical impedance spectroscopy (EIS) was performed in 0.1 M PBS (pH 7.4) containing 5 mM $[\text{Fe}(\text{CN})_6]^{3-/4-}$ (1:1) and 10 mM KCl in the frequency range from 0.1 Hz to 100 kHz with 5 mV as the amplitude at a polarization potential of 0.18 V. All measurements were repeated for a minimum of three times with separate electrodes to obtain statistically meaningful results.

Results and discussion

Mechanism of duplex-like DNA structure for Ag^+ ions detection

Scheme S-1 illustrates the mechanism of this biosensor. The single strand oligonucleotide S1 anchored the composite GNPs/MCN/L-Lys/GCE platform by Au-S covalent bond, ready for the hybridization with S2 and S3 to form a stable hairpin structure. $[\text{Fe}(\text{CN})_6]^{3-/4-}$, a redox pair, is frequently used as a redox indicator for the electrode kinetics at the interface (as shown in Scheme S-1). Upon the hybridization of surface-tethered probe DNA with its complementary probes in solution, the interfacial charge-transfer resistance for the negatively

charged $[\text{Fe}(\text{CN})_6]^{3-/4-}$ redox probe on the electrode is remarkably increased due to the formation of hairpin structure. Then the interfacial charge-transfer resistance as the hairpin structure is changed to duplex-like structured upon DNA interaction with Ag^+ in solution to form a C- Ag^+ -C complex at electrode surface. Fig. 1 shows the representative Nyquist plots of the EIS spectra of before and after hybridization with probes (S1+S2+S3), and after incubation in the solution of 0 M Ag^+ (Fig. 1A) and 10^{-5} M Ag^+ (Fig. 1B), respectively. It can be clearly observed that the impedance increased after hybridization with probes (S1+S2+S3) and shift back in the presence of Ag^+ (10^{-5} M). In fact, the difference of the charge transfer resistance (ΔR_{ct}) of DNA films in the presence and absence of the metal ion was dependent on the concentration of the given metal ion²⁹. The result also coincides with the presumptive mechanism about the silver induced conformational change of hairpin structure to duplex-like structure, thus enhancing the electron transfer. The different charge and conformational characteristics of DNA on the surface led to different charge-transfer resistances for the redox indicator ions^{29, 30}. On the basis of the results discussed above, the interactions between DNA and Ag^+ led to the decrease of R_{ct} which could be used for the detection of Ag^+ .

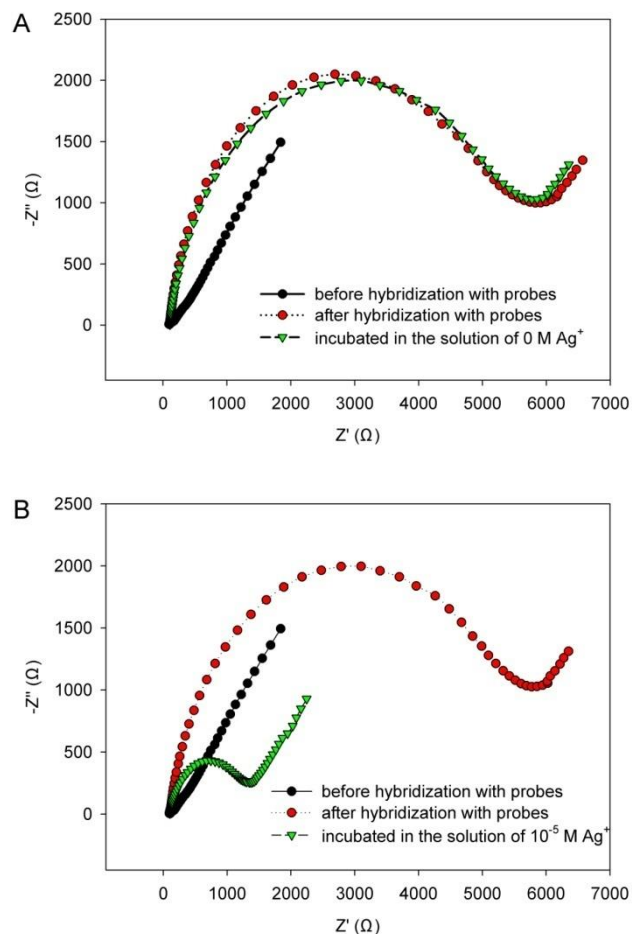


Fig. 1 Nyquist plots for the Faradaic impedance measurement before and after hybridization with probes (S1+S2+S3), and after incubation in the solution of (A) 0 M and (B) 10^{-5} M Ag^+ in PBS (0.1 M, pH 7.4) containing 5 mM $[\text{Fe}(\text{CN})_6]^{3-/4-}$ (1:1) and 10 mM KCl, in the frequency range from 0.1 Hz to 100

kHz with 5 mV as the amplitude at a polarization potential of 0.18 V.

Characterization of MNC and electrode assembly process

The SEM and TEM images of MCN are shown in Fig. S–2. As seen in Fig. S–2A, MCN formed a chained rod structure that was evenly dispersed on the surface of GCE. Fig. S–2B clearly presented a hexagonal arrangement of the mesopores. Besides, the Fourier–transform infrared (FT–IR) spectrum, was presented in our previous work²³, the result showed that the MCN was enriched in amino. Thus, the amino group could make the MCN/L–Lysine more stable.

To test the performance of the modified electrode, CV was carried out in phosphate buffer (pH 7.4) containing 5 mM [Fe(CN)₆]^{3–/4–} (1:1) and 10 mM KCl to test the property of the modified electrode. As seen in Fig. 2, the immobilization of L–Lys on the GCE led to a significant decrease in peak current of the redox probe. After modification with MCN and GNPs, the peak current increased obviously and the peak potential difference reached the minimum. These cyclic voltammograms proved that the modified electrode had a good current response capability.

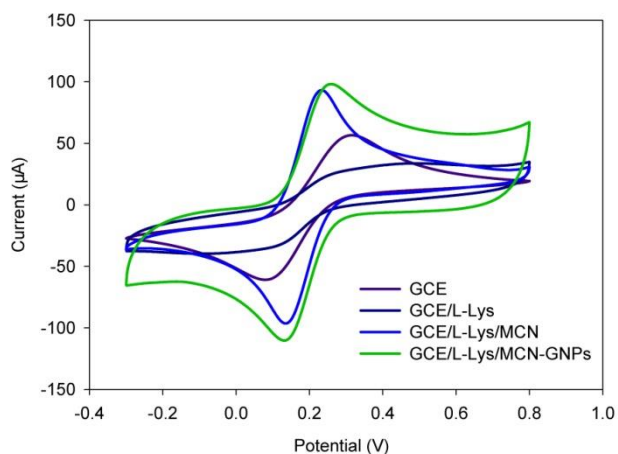


Fig. 2 Cyclic voltammetry diagrams of GCE, GCE/L–Lys, GCE/L–Lys/MCN, GCE/L–Lys/MCN–GNPs, using a 10.0 mM KCl solution containing 5.0 mM [Fe(CN)₆]^{4–/3–}, with potential range of –0.3 to 0.8 V, and a scan rate of 100 mV s^{–1}.

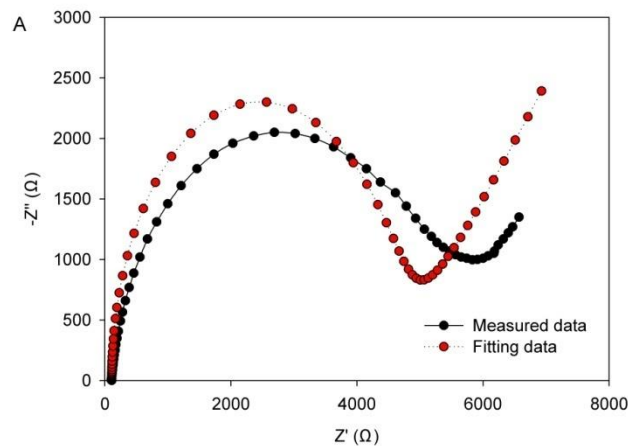
Optimization of the variables of experimental conditions

The experimental conditions were optimized before the quantitative analysis of Ag⁺. Fig. S–3A demonstrated the effect of self–assembly time of capture probe (S1) on the modified electrode surface. The ΔR_{ct} increased with the self–assembly time, and then reached a plateau at 10 h. Therefore, the self–assembly time of 10 h was used in the subsequent measurements. Similarly, the optimization of hybridization conditions includes hybridization time of DNA hybridization (S2+S3) reaction. The hybridization time is an important factor to ensure the adequacy of a contact reaction. The response current increased sharply with the hybridization time increasing from 30 to 60 min, then leveling off (Fig. S–3B). The time–course of the Ag⁺ complexing with C bases is studied by the electrochemical response signal to optimize the time so as to

obtain the maximum loading of Ag⁺ on the sensor interface (Fig. S–3C). The experimental data indicates that incubation time has a great effect on the response signal, which implies that the adsorption quantity of Ag⁺ relies much on the time accretion. The ΔR_{ct} was enlarged with the incubation time increasing and remain constant at a saturation value after about 120 min, indicating that 120 min as the incubation time is absolutely efficient. Accordingly, the sensor was incubated in Ag⁺ ion solution for 120 min in all subsequent analyses.

Analytical properties of the impedimetric DNA biosensor

The measured EIS data can be fitted with an equivalent circuit as shown in Scheme S–1c. This equivalent circuit consists of the electron–transfer resistance (R_{ct}), the warburg impedance (Z_w), the ohmic resistance of the electrolyte (R_s), and interfacial capacitance (C_{dl}). EIS includes a semicircular part and a linear part. The semicircle diameter could represent the electron–transfer resistance, R_{ct} , which is the polarization resistance at an equilibrium potential, is utilized as a main indicator in the EIS detection. The measured data and the fitting curve shown in the Fig. 3 are the EIS fitting plots of the electrode (after hybridization with S1+S2+S3) using the above equivalent circuit shown in Scheme S–1c. The various elements of the equivalent circuit were obtained and the plot fitting and the fitting errors were less than 6.0%. The good agreement between the measured data and the fitting curve indicates that this equivalent circuit is suitable and meaningful for this electrochemical system. Therefore, this equivalent circuit is used to fit the impedance spectroscopy data and extract the values of the equivalent circuit elements. The impedance spectra for all the system were analyzed with the help of Randles equivalent circuit.



Analyst

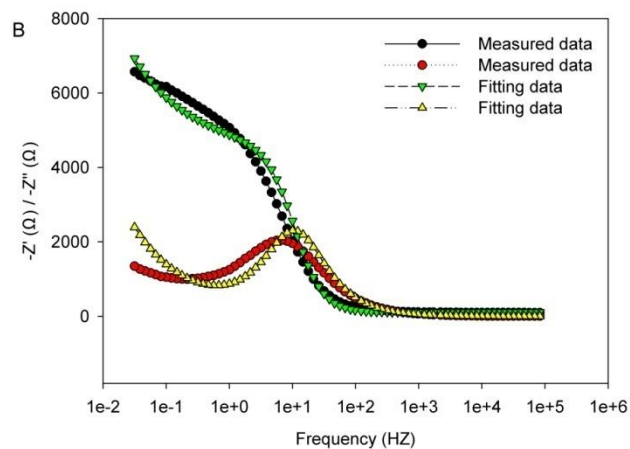


Fig. 3 (A) Nyquist plots of electrochemical impedance spectroscopy of the electrode (after hybridization with S1+S2+S3) together with the fitting data. (B) Real and Imag plots of electrochemical impedance spectroscopy of the electrode (after hybridization with S1+S2+S3).

Fig. 4A displays the Nyquist plots obtained with the modified electrode in 0.1 M PBS (pH 7.4) containing 5 mM $[\text{Fe}(\text{CN})_6]^{3-/4-}$ (1:1) and 10 mM KCl after the electrode was incubated with different concentrations of Ag^+ under the optimized experimental conditions (as shown in Fig. S-3). As shown in Fig. 4A, upon decreasing the concentration of Ag^+ from 10^{-10} M to 10^{-5} M, only part of C-C mismatches could react with Ag^+ to form C- Ag^+ -C, which led to the decrease in ΔR_{ct} (as shown in Table S-1). The change in the R_{ct} was linear with the logarithm of the concentration of Ag^+ within a concentration range from 10^{-10} M to 10^{-5} M. The linear regression equation was $Y = (-592.0143 \pm 43.9328)X + (6759.2571 \pm 337.9304)$ (Y is the ΔR_{ct} (Ω), X is the common logarithmic value of the target concentration (M)) with a correlation coefficient $R^2=0.97$. The detection limit of the impedimetric DNA biosensor was estimated to be 5×10^{-11} M, based on $S/N=3$. The proposed biosensor exhibited improved analytical performances in terms of linear detection range, and showed lower detection limit. The limit of detection was competitive with other highly sensitive detection approaches such as fluorescence, colorimetry and electrochemical methods, as presented in Table 1.

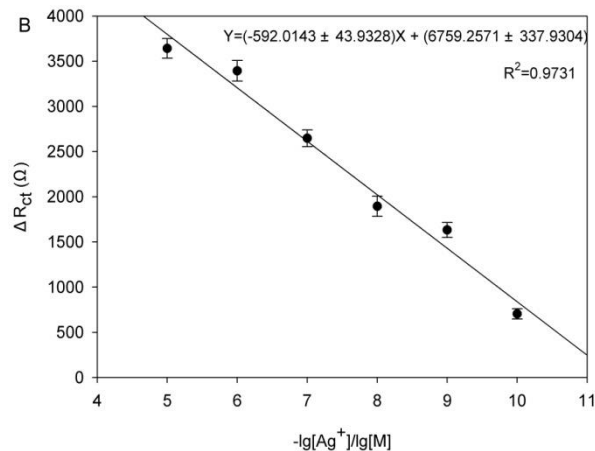
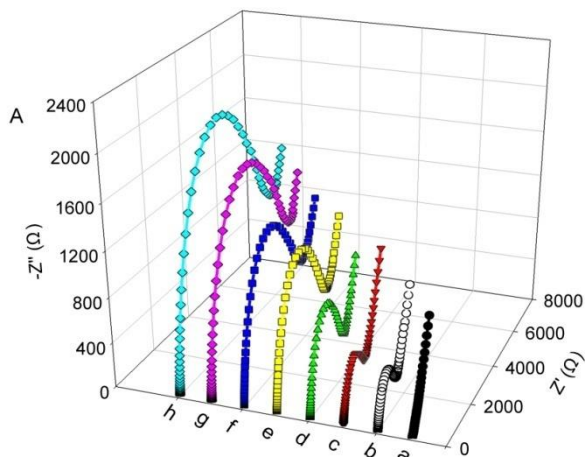


Fig. 4 (A) A series of Nyquist plots before hybridization (a), after hybridization with DNA (S1+S2+S3) and incubation in 1×10^{-5} M (b), 1×10^{-6} M (c), 1×10^{-7} M (d), 1×10^{-8} M (e), 1×10^{-9} M (f) and 1×10^{-10} M (g) Ag^+ , and after hybridization with DNA (S1+S2+S3) (h). (B) The plot of ΔR_{ct} vs. Ag^+ concentration ranging from 1×10^{-10} M– 1×10^{-5} M. Error bars indicate standard deviations from three replicative tests.

The stability, reproducibility and selectivity of the biosensor

The repeatability of the same biosensor was examined by detecting 1×10^{-8} M Ag^+ in 0.1 M PBS (pH 7.4) containing 5 mM $[\text{Fe}(\text{CN})_6]^{3-/4-}$ (1:1) and 10 mM KCl using EIS technique (as shown in Fig. 5). A relative standard deviation (R.S.D.) value of 4.1% was obtained for three determinations, which implied a good repeatability of the measurements with no need to apply a complicated pretreatment procedure to the electrode.

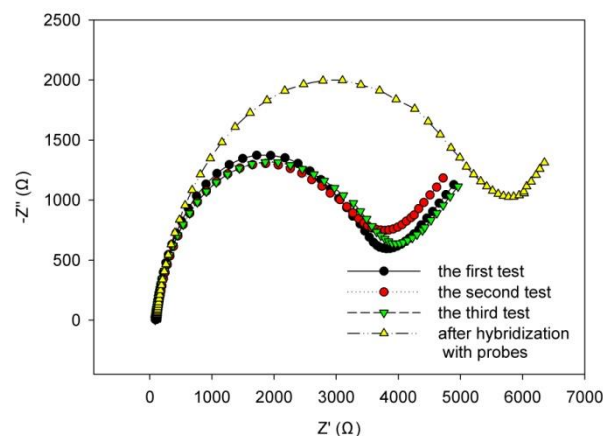


Fig. 5 The repeatability of the same biosensor for 1.0×10^{-8} M Ag^+ (different line represents different testing sample with the same biosensor).

The reproducibility was also investigated with five different GCEs constructed by the same steps independently, as presented in Fig. S-4. The RSD was 4.4% for the ΔR_{ct} to 1×10^{-8} M Ag^+ , indicating that the fabrication procedure was reliable,

Table 1 Comparison with other published Ag⁺ detection sensor.

method	Materials	Linear range (mol L ⁻¹) ¹⁾	LOD (mol L ⁻¹)	References
The red-shift of the emission band of quantum dots (QDs)	CdTe	1.5×10 ⁻⁵ –1×10 ⁻⁷	5×10 ⁻⁸	31
Impedimetric immobilized DNA-based sensor for the detection of Ag ⁺	Gold electrode	1×10 ⁻⁷ –8×10 ⁻⁷	1×10 ⁻⁸	29
Colorimetric and ratiometric fluorescent chemosensor for the selective detection of Ag ⁺	Heptamethine cyanine	6×10 ⁻⁸ –5×10 ⁻⁶	6×10 ⁻⁸	32
Electrochemical sensing platform for Ag ⁺ detection	Multi-walled carbon nanotubes	1×10 ⁻⁸ –5×10 ⁻⁷	1.3×10 ⁻⁹	33
Colorimetric detection of Ag ⁺	Gold nanoparticles	—	3.3×10 ⁻⁹	34
Oligonucleotide-based fluorogenic probe	Sybr Green I	5×10 ⁻⁸ –7×10 ⁻⁷	3.2×10 ⁻⁸	35
Magnified fluorescence detection of Ag ⁺	nano-graphite–DNA hybrid and DNase I	—	3×10 ⁻¹⁰	12
Colorimetric detection of Ag ⁺	Hemin DNase I	—	6.3×10 ⁻⁹	36
Ion-Selective Electrodes detection of Ag ⁺	Ionophore-Doped Fluorous Membranes	—	3.8×10 ⁻¹¹	38
A Nanoparticle Autocatalytic Sensor for Ag ⁺ detection	o-phenylenediamine	6×10 ⁻⁸ –6×10 ⁻⁵	6×10 ⁻⁸	37
Impedimetric Biosensor based on duplex-like DNA scaffolds	Ordered Mesoporous Carbon Nitride	10 ⁻¹⁰ –10 ⁻⁵	5×10 ⁻¹¹	This work

and the modified GCE had good reproducibility. The long-term stability of the biosensor was explored. It was investigated through the response to 1×10⁻⁸ M Ag⁺ in 0.1 M PBS (pH 7.4) containing 5 mM [Fe(CN)₆]^{3-/4-} (1:1) and 10 mM KCl for 1 month. When not in use, the electrode was stored in a moist state at 4 °C, and the current response was periodically measured. Beyond this period, the experiment was carried out per 10 days. The result showed that the biosensor retained about 85% of its original ΔR_{ct} after 1 month. The relatively good stability of the biosensor may be explained by the fact that the film (MCN and GNPs) could provide a biocompatible microenvironment, and the hairpin structure and the specific recognition ability to form C–Ag⁺–C could be protected effectively.

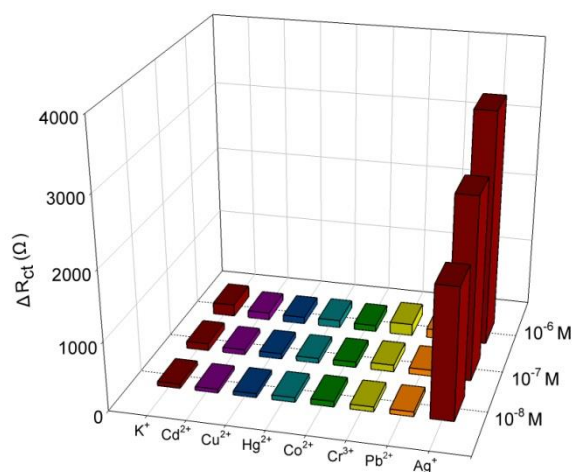


Fig. 6 Selectivity and interference study in the analysis of Ag⁺ by the duplex-like DNA system. The data were averages of three replicate measurements.

Selectivity of this detection method is tested by substituting the Ag⁺ in the system with various metal ions which are commonly present in real samples, such as Pb²⁺, Cr³⁺, Co²⁺, Hg²⁺, Cu²⁺, Cd²⁺ and K⁺. As shown in Fig. 6, each competing metal ion is

tested at 1×10⁻⁶ M, 1×10⁻⁵ M, 1×10⁻⁴ M under the same experimental conditions. None of the corresponding ΔR_{ct} of the tested metal ions was higher than half of that produced by 1×10⁻⁸ M, 1×10⁻⁷ M, 1×10⁻⁶ M Ag⁺. Such excellent selectivity is attributed to the specific C–Ag⁺–C base pairing which relates closely with signal change as mentioned above. The proposed biosensor exhibited good anti-interference ability and provided the potential to selectively determine Ag⁺ levels in real samples.

Real samples detection

Five sewage samples were collected respectively from a discharge outlet of untreated domestic sewage on the bank of Xiangjiang River, Hunan Province, and then were filtered through a 0.2 μm membrane to remove oils and other organic impurities. Subsequently, the sewage samples were spiked with standard solutions of Ag⁺ over the concentration range from 0.5 to 5000 nM prior to measurement. As seen in Table S–2, the recoveries ranging from 95.2% to 105.8% after standard additions are satisfactory, suggesting that the biosensor could be efficiently used for the detection of Ag⁺ content in the real samples.

Conclusions

In this paper, an unlabeled immobilized DNA-based sensor was reported to detect Ag⁺ through the difference in charge-transfer resistance (ΔR_{ct}) before and after DNA interactions with Ag⁺, which were monitored by electrochemical impedance spectroscopy (EIS). ΔR_{ct} is sufficiently sensitive to detect Ag⁺ as low as 5×10⁻¹¹ M with the linear range from 10⁻¹⁰ M to 10⁻⁵ M. Moreover, because of the signal amplification by the MCN and GNPs platform and excellent specificity resulting from the hairpin DNA-based probes and the C–Ag⁺–C interaction, the sensor maintained high selectivity over other nonspecific metal ions. It has good potential for application in environmental monitoring. Furthermore, alternative sensing devices for other metal ions may be developed as well using other natural or synthetic specific hairpin probes.

Acknowledgements

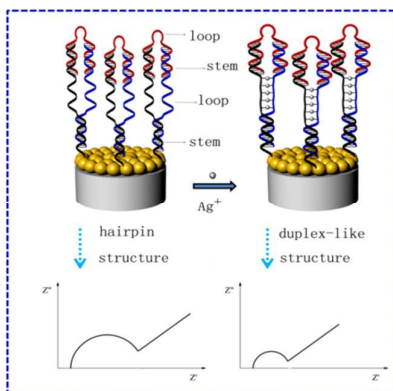
The study was financially supported by the Young Top–Notch Talent Support Program of China (2012), the National Natural Science Foundation of China (51222805), the Program for New Century Excellent Talents in University from the Ministry of Education of China (NCET–11–0129), Interdisciplinary Research Project of Hunan University, China Scholarship Council (CSC) (2010843195), the Fundamental Research Funds for the Central Universities, Hunan University, and Hunan Provincial Innovation Foundation For Postgraduate (CX2009B080).

Notes and references

^a Hunan University, College of Environmental Science and Engineering Changsha, 410082, China.

^b Key Laboratory of Environmental Biology and Pollution Control, Hunan University, Ministry of Education, Changsha 410082, P.R. China. E-mail: tanglin@hnu.edu.cn(L. Tang), zgmiming@hnu.edu.cn(G.M. Zeng) Electronic Supplementary Information (ESI) available: More details about the optimization of DNA–based biosensor, the reproducibility of the biosensor, electrodeposition of L–Lys, analysis the Ag⁺ in real samples, SEM and TEM images of MCN. See DOI: 10.1039/b000000x/

- 1 J. M. Liu, L. p. Lin, X. X. Wang, S. Q. Lin, W. L. Cai, L. H. Zhang and Z. Y. Zheng, *Analyst*, 2012, **137**, 2637–2642.
- 2 T.W. Purcell and J.J. Peters, *Environmental Toxicology and Chemistry*, 1998, **17**, 539–546.
- 3 S. Kim, J. E. Choi, J. Choi, K. H. Chung, K. Park, J. Yi and D. Y. Ryu, *Toxicology in vitro*, 2009, **23**, 1076–1084.
- 4 J. L. Manzoori, H. Abdolmohammad–Zadeh and M. Amjadi, *Journal of hazardous materials*, 2007, **144**, 458–463.
- 5 S. Ashoka, B. M. Peake, G. Bremner, K. J. Hageman and M. R. Reid, *Analytica chimica acta*, 2009, **653**, 191–199.
- 6 P. R. Aranda, P. H. Pacheco, R. A. Olsina, L. D. Martinez and R. A. Gil, *Journal of Analytical Atomic Spectrometry*, 2009, **24**, 1441–1445.
- 7 N. Pourreza, H. Parham, A. Kiasat, K. Ghanemi and N. Abdollahi, *Talanta*, 2009, **78**, 1293–1297.
- 8 I. Willner and M. Zayats, *Angewandte Chemie International Edition*, 2007, **46**, 6408–6418.
- 9 Y. Tanaka, S. Oda, H. Yamaguchi, Y. Kondo, C. Kojima and A. Ono, *Journal of the American Chemical Society*, 2007, **129**, 244–245.
- 10 T. Li, S. Dong and E. Wang, *Journal of the American Chemical Society*, 2010, **132**, 13156–13157.
- 11 A. Ono, S. Cao, H. Togashi, M. Tashiro, T. Fujimoto, T. Machinami, S. Oda, Y. Miyake, I. Okamoto and Y. Tanaka, *Chemical communications*, 2008, **39**, 4825–4827.
- 12 Y. Wei, B. Li, X. Wang and Y. Duan, *Biosensors and Bioelectronics*, 2014, **58**, 276–281.
- 13 G. Xu, G. F. Wang, X. P. He, Y. H. Zhu, L. Chen and X. J. Zhang, *Analyst*, 2013, **138**, 6900–6906.
- 14 G. Liu, Y. Wan, V. Gau, J. Zhang, L. Wang, S. Song and C. Fan, *Journal of the American Chemical Society*, 2008, **130**, 6820–6825.
- 15 S. Y. Niu, Q. Y. Li, R. Ren and S. S. Zhang, *Biosensors and Bioelectronics*, 2009, **24**, 2943–2946.
- 16 P. Riccelli, F. Merante, K. Leung, S. Bortolin, R. Zastawny, R. Janeczko and A. S. Benight, *Nucleic acids research*, 2001, **29**, 996–1004.
- 17 C. C. Chang, S. Lin, S. C. Wei, C. Y. Chen and C. W. Lin, *Biosensors and Bioelectronics*, 2011, **30**, 235–240.
- 18 G. Xu, G. F. Wang, Y. H. Zhu, L. Chen, X. P. He, L. Wang and X. J. Zhang, *Biosensors and Bioelectronics*, 2014, **59**, 269–275.
- 19 G. P. Yan, Y. H. Wang, X. X. He, K. M. Wang, J. Su, Z. F. Chen and Z. H. Qing, *Talanta*, 2012, **94**, 178–183.
- 20 S. H. Lee, C. K. Lee, S. R. Shin, B. K. Gu, S. Kim, T. M. Kang and S. J. Kim, *Sensors and Actuators B*, 2010, **145**, 89–92.
- 21 L. J. Yan, X. J. Bo, Y. F. Zhang and L. P. Guo, *Electrochimica Acta*, 2014, **137**, 693–699.
- 22 L. P. Lu, L. H. Xu, T. F. Kang and S. Y. Cheng, *Applied Surface Science*, 2013, **284**, 258–262.
- 23 Y. Y. Zhou, L. Tang, G. M. Zeng, J. Chen, Y. Cai, Y. Zhang, G. D. Yang, Y. Y. Liu, C. Zhang and W. W. Tang, *Biosensors and Bioelectronics*, 2014, **61**, 519–525.
- 24 L. Tang, Y. Y. Zhou, G. M. Zeng, Z. Li, Y. Y. Liu, Y. Zhang, G. Q. Chen, G. D. Yang, X. X. Lei and M. S. Wu, *Analyst*, 2013, **138**, 3552–3560.
- 25 Y. Y. Zhou, L. Tang, G. M. Zeng, Y. Zhang, Z. Li, Y. Y. Liu, J. Chen, G. D. Yang, L. Zhou and S. Zhang, *Analytical Methods*, 2014, **7**, 2371–2378.
- 26 Y. Zhang, G. M. Zeng, L. Tang, Y. P. Li, L. J. Chen, Y. Pang, Z. Li, C. L. Feng and G. H. Huang, *Analyst*, 2011, **136**, 4204–4210.
- 27 T. H. M. Kjörlman, H. Peng, C. Soeller and J. Travas-Sejdic, *Analytical chemistry*, 2008, **80**, 9460–9466.
- 28 L. Tang, G. M. Zeng, G. L. Shen, Y. P. Li, C. Liu, Z. Li, J. Luo, C. Z. Fan, C. P. Yang, *Biosensors and Bioelectronics*, 2009, **24**, 1474–1479.
- 29 Z. Lin, X. Li and H. B. Kraatz, *Analytical chemistry*, 2011, **83**, 6896–6901.
- 30 Y. Wang, C. Li, X. Li, Y. Li and H. B. Kraatz, *Analytical chemistry*, 2008, **80**, 2255–2260.
- 31 J. Wang, J. Liang, Z. Sheng and H. Han, *Microchimica Acta*, 2009, **167**, 281–287.
- 32 H. Zheng, M. Yan, X. X. Fan, D. Sun, S. Y. Yang, L. J. Yang, J. D. Li and Y. B. Jiang, *Chemical Communications*, 2012, **48**, 2243–2245.
- 33 G. Yan, Y. Wang, X. He, K. Wang, J. Su, Z. Chen and Z. Qing, *Talanta*, 2012, **94**, 178–183.
- 34 Y. M. Sung and S. P. Wu, *Sensors and Actuators B: Chemical*, 2014, **197**, 172–176.
- 35 Y. H. Lin and W. L. Tseng, *Chemical Communications*, 2009, **43**, 6619–6621.
- 36 X. H. Zhou, D. M. Kong and H. X. Shen, *Analytica chimica acta*, 2010, **678**, 124–127.
- 37 X. Yang and E. Wang, *Analytical chemistry*, 2011, **83**, 5005–5011.
- 38 C. Z. Lai, M. A. Fierke, R. C. da Costa, J. A. Gladysz, A. Stein and P. Bühlmann, *Analytical chemistry*, 2010, **82**, 7634–7640.



An unlabeled immobilized DNA-based biosensor with MCN for detection of Ag^+ by EIS with $[Fe(CN)_6]^{4-/3-}$ as a redox couple.